Bioorganic & Medicinal Chemistry 18 (2010) 5081–5089

Contents lists available at ScienceDirect

Bioorganic & Medicinal Chemistry

journal homepage: www.elsevier.com/locate/bmc

# Pteridine–sulfonamide conjugates as dual inhibitors of carbonic anhydrases and dihydrofolate reductase with potential antitumor activity

Sérgio M. Marques [a], Éva A. Enyedy [a], Claudiu T. Supuran [b], Natalia I. Krupenko [c], Sergey A. Krupenko [c], M. Amélia Santos [a,*]

[a] Instituto Superior Técnico, Centro de Química Estrutural, Av. Rovisco Pais 1, 1049-001 Lisboa, Portugal
[b] Università degli Studi di Firenze, Laboratorio di Chimica Bioinorganica, Rm. 188, Via della Lastruccia 3, I-50019 Sesto Fiorentino (Firenze), Italy
[c] Medical University of South Carolina, Department of Biochemistry and Molecular Biology, Charleston, SC 29425, USA

ARTICLE INFO

*Article history:*
Received 8 February 2010
Revised 24 May 2010
Accepted 26 May 2010
Available online 2 June 2010

*Keywords:*
Multi-target drugs
Dihydrofolate reductase inhibitors
Carbonic anhydrase inhibitors
Cancer therapy

ABSTRACT

Recent evidences suggest that cancer treatment based on combination of cytostatic and conventional chemostatic therapeutics, which are usually cytotoxic, can provide an improved curative option. On the sequence of our previous work on methotrexate (MTX) derivatives, we have developed and evaluated novel MTX analogues, containing a pteridine moiety conjugated with benzenesulfonamide derivatives, thus endowed with the potential capacity for dual inhibition of dihydrofolate reductase (DHFR) and carbonic anhydrases (CA). These enzymes are often overexpressed in tumors and are involved in two unrelated cellular pathways, important for tumor survival and progression. Their simultaneous inhibition may turn beneficial in terms of enhanced antitumor activity.

Herein we report the design and synthesis of several diaminopteridine–benzenesulfonamide and -benzenesulfonate conjugates, differing in the nature and size of the spacer group between the two key moieties. The inhibition studies performed on a set of CAs and DHFR, revealed the activities in the low nanomolar and low micromolar ranges of concentration, respectively. Some inhibitors showed selectivity for the tumor-related CA (isozyme IX). Cell proliferation assays using two tumor cell lines (the non-small cell lung carcinoma, A549, and prostate carcinoma, PC-3) showed activities only in the millimolar range. Nevertheless, this fact points out the need of improving the cell intake properties of these new compounds, since the general inhibitory profiles revealed their potential as anticancer agents.



## 1. Introduction

Since most cancers proved to often evade the conventional chemotherapeutic treatments, the combination of several anticancer treatments has been one of the recent medical research strategies, along with the search for new targets. There is worldwide interest towards the development of multifunctional and multitargeting drugs, which is an alternative to drug combination protocols for the treatment of diseases with complex etiologies (such as cancer).[1,2] This trend has also challenged us to embark on the development and study of new potential drugs with dual activity against cancer pathways.[3,4] The antifolate methotrexate (MTX, see Fig. 1) is the oldest and one of the most widely used anticancer drugs. Its activity is based on blockage of folate pathways, important for cancer cell survival, by inhibiting dihydrofolate reductase (DHFR).[5,6] Another pathway, which might be relevant to malignant proliferation, involves carbonic anhydrases (CAs). Recent studies revealed that CA isozymes IX, XII, and CA-related protein VIII are highly abundant in tumors and are involved in tumorigenesis and tumor progression,[7,8] and that has led to their validation as new therapeutic targets for cancer chemotherapy intervention.[9,10] Thus, we have pursued a research strategy focused on the novel hybrid compounds with potential dual inhibitory activity against DHFR and CAs. For this purposed, two key chemical moieties (a pteridine and a benzenesulfonamide) are combined in the same molecular entity for blocking the function of the enzymes from two unrelated metabolic pathways involved in tumor progression, with expected beneficial in terms of enhancing the antitumor activity.

We present herein the design and synthetic route of several arylsulfonamide- and arylsulfonate–diaminopteridine conjugates, which differ in the length and the nature of spacer (linker) between the two molecular moieties (pteridine and benzenesulfonyl groups, see Chart 1). The inhibitory activities of these compounds against three carbonic anhydrase isoforms (CA I, II and IX) and DHFR, as well as their antiproliferative activities in the A549 (non-small cell lung carcinoma) and PC-3 (prostate carcinoma) cell lines, are also presented and discussed.

* Corresponding author. Tel.: +351 218419273; fax: +351 218464455.
*E-mail address:* masantos@ist.utl.pt (M. Amélia Santos).

0968-0896/$ - see front matter © 2010 Elsevier Ltd. All rights reserved.
doi:10.1016/j.bmc.2010.05.072

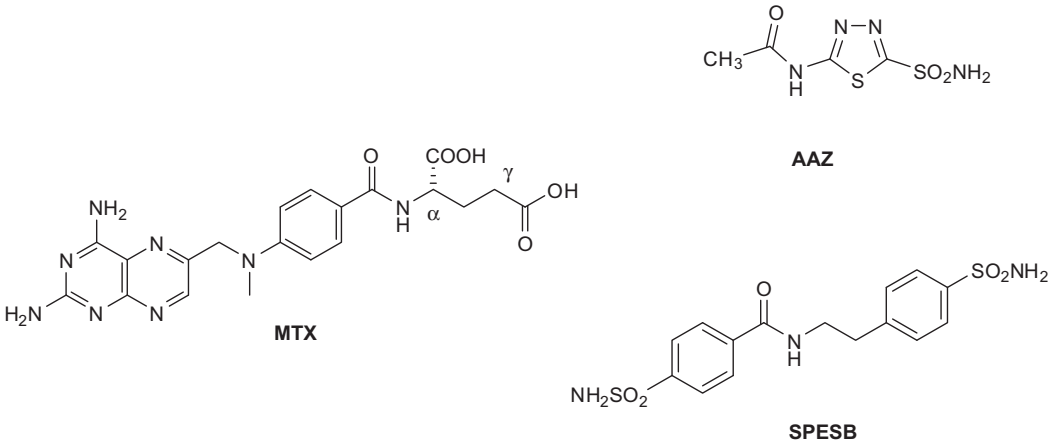


**Figure 1.** Structures of methotrexate (MTX, a DHFR inhibitor and current antitumor drug), and of reference CA inhibitors: acetazolamide (AAZ) and *N*-(4-sulfamoylphenylethyl)-4-sulfamoylbenzamide (SPESB).

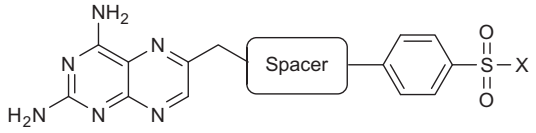


| Compound | Spacer | X |
|---|---|---|
| **1a** | -NH- | $NH_2$ |
| **1b** | -NH- | OH |
| **2a** | -NH-$CH_2CH_2$- | $NH_2$ |
| **2b** | -NH-$CH_2CH_2$- | OH |
| **3a** | -*p*ABA-NH$CH_2CH_2$- | $NH_2$ |
| **3b** | -*p*ABA-NH-$CH_2CH_2$- | OH |
| **4a** | -NMe*p*ABA-NH$CH_2CH_2$- | $NH_2$ |

*p*ABA = -NH-Ph-CO-

NMe*p*ABA = -$NCH_3$-Ph-CO-

**Chart 1.**

## 2. Chemistry

For the preparation of the new inhibitors, the benzenesulfonyl-containing moieties were coupled to the 2,4-diamino-6-(hydroxymethyl)pteridine (PtOH). This was carried out in two main steps: firstly, PtOH was treated with thionyl bromide, to give the corresponding halogenated analogue (PtBr). Afterwards, an amine-containing derivative having the benzenesulfonyl moiety attached was coupled with the pteridine moiety via nucleophilic substitution at PtBr under strictly anhydrous conditions, yielding the final compounds. This synthetic route is shown in Scheme 1 for compounds **1** and **2** (**a** and **b** analogues).

In the case of the *p*-aminobenzoyl (*p*ABA)- or *N*-methyl-*p*-aminobenzoyl (*N*Me*p*ABA)-containing inhibitors (compounds **3a**–**4a**, and **3b**), before the coupling to the pteridine moiety, the benzenesulfonyl-containing intermediates were previously synthesized through different steps (see Scheme 2). The *p*ABA amine group was first protected with the *tert*-butoxycarbonyl (*Boc*) group, yielding compound **5**. *Boc*-*p*ABA (**5**) and *N*Me*p*ABA were then conjugated with the sulfonamide- (or sulfonate-) containing fragments, via the TBTU-activation of the corresponding carboxylic groups, generating compounds **6** (**a, b**) and **8**. After the *Boc*-deprotection of **6** with TFA, to afford the respective amines, **7** and **8** were coupled with the halogenated pteridine, PtBr, as described for compounds **1** and **2**, in order to obtain the target compounds.

## 3. Results and discussion

### 3.1. Enzyme inhibition

The new compounds were tested in terms of their inhibitory activities towards a set of physiologically relevant human carbonic anhydrases (the ubiquitous CA I and II, and the tumor-associated isoform CA IX) and dihydrofolate reductase (DHFR). Results of these bioassays are presented in Table 1. Our data demonstrated that most of the new compounds inhibited the tested enzymes, but the activities vary from the low nanomolar to the micromolar range.

Regarding the CAs inhibition profile, all compounds displayed moderate activity with CA I ($K_I$ values ranging from 1.2 to 36 μM), as compared with reference inhibitors ($K_I$ values of 250

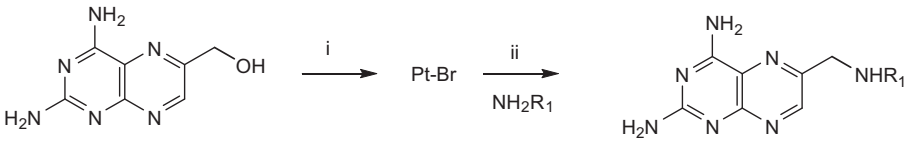


**Pt-OH**

$R_1$ = -$PhSO_2X$ **(1)**
-$(CH_2)_2PhSO_2X$ **(2)**

X = $NH_2$ **(a)**
OH **(b)**

**Scheme 1.** Synthesis of compounds **1** and **2** (**a** and **b** analogues). Reagents and conditions: (i) $SOBr_2$, rt; (ii) NaH, $CaCO_3$, DMF, rt.

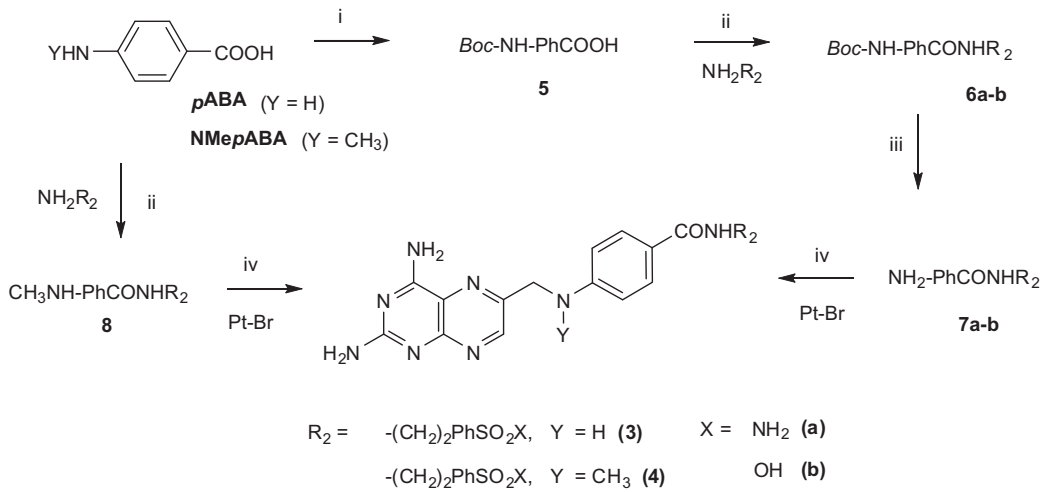


**Scheme 2.** Synthesis of compounds **3a**, **3b**, and **4a**. Reagents and conditions: (i) $Boc_2O$, $Na_2CO_3$, $H_2O$/dioxane, rt; (ii) TBTU, NMM, DMF, 0 °C; (iii) 50% TFA, $CH_2Cl_2$, rt; (iv) NaH, $CaCO_3$, DMF, rt.

**Table 1**
Activities of the reference inhibitors AAZ, SPESB, MTX, and the synthesized compounds toward human CA I, II, IX, and DHFR, compared to their respective antiproliferative effects in A549 and PC-3 cancer cells lines

| Compound[a] | | | $K_I$ (nM) | | | *Select. CA IX/II* | $IC_{50}$ (nM) | | |
|---|---|---|---|---|---|---|---|---|---|
| | Spacer | X | CA I | CA II | CA IX | | DHFR | A549 | PC-3 |
| **1a** | NH | $NH_2$ | 1150 | 4.5 | 2.1 | *2.2* | 2500 | $5 \times 10^6$ | $0.55 \times 10^6$ |
| **1b** | NH | OH | 2170 | 350 | >1000 | *<0.35* | 2000 | $6 \times 10^6$ | $0.5 \times 10^6$ |
| **2a** | $NHCH_2CH_2$ | $NH_2$ | 27,400 | 45.0 | 4.7 | *9.6* | n.a.[b] | $3 \times 10^6$ | $0.3 \times 10^6$ |
| **2b** | $NHCH_2CH_2$ | OH | 8170 | 26,400 | >1000 | *<2.6* | n.a.[b] | $1 \times 10^6$ | $0.46 \times 10^6$ |
| **3a** | *p*ABA–NH–$CH_2$–$CH_2$ | $NH_2$ | 3560 | 920 | 2.5 | *369* | 20,000 | $2 \times 10^6$ | $0.4 \times 10^6$ |
| **3b** | *p*ABA–NH–$CH_2$–$CH_2$ | OH | 36,400 | 37,100 | >1000 | *<3.7* | 1300 | $5 \times 10^6$ | $0.5 \times 10^6$ |
| **4a** | NMe*p*ABA-NH–$CH_2$–$CH_2$ | $NH_2$ | 1290 | 260 | 3.7 | *70* | 1800 | $6 \times 10^6$ | $0.5 \times 10^6$ |
| AAZ | | | 250 | 12 | 25 | *0.48* | | | |
| SPESB | | | 40 | 5 | 18 | *0.28* | | | |
| MTX | | | | | | | 5 | 5 | 1 |

[a] With the formula as in Chart 1.
[b] n.a. means no inhibition at 0.5 mM.

and 40 nM, for AAZ and SPESB, respectively, see Fig. 1). This is a good feature of these compounds, as CA I is an off target enzyme. Concerning the inhibition of isozyme CA II, the activities presented a more pronounced variations, the highest activities being observed for compounds **1a** and **4a**, with $K_I$ of 4.5 and 260 nM, respectively, and the lowest for **3b**, with 37 μM. For this isoform, it was clear the activity dependency on the nature of the benzenesulfonyl moiety present in the inhibitor, the benzenesulfonamide analogues (–$PhSO_2NH_2$) being more active than their sulfonic acid homologues ($PhSO_3H$) (i.e., compounds **1a** vs **1b**, **2a** vs **2b** and **3a** vs **3b**). This behaviour was expected and is according to the literature;[11,12] in fact, it is well known that the aromatic sulfonamides are able to establish stronger interactions with the active site of the CAs than most of other zinc-binding groups (ZBG). This feature is due to the coordination of the catalytic zinc(II) ion by the N-atom of the sulfonamide moiety, and the formation of two H-bonds between the threonine residue in the vicinity of that metal ion with the sulfonamide $SO_2NH_2$ group.[13] The activity of the inhibitors towards CA II also decreased with increasing of the spacer's length (i.e., following this order in the series **1a**, **2a**, and **3a**). However, compound **4a** revealed higher affinity for this enzyme than **3a**, thus indicating that the *N*-methyl group on the *p*ABA spacer should provide some extra lipophilic binding interactions. Comparison with the reference inhibitors shows that only compound **1a** is slightly more active than AAZ and SPESB ($K_I$ of 4.5, 12 and 5 nM, respectively), suggesting that the 2,4-diamino-6-methylpteridine moiety interacts favourably within the CA II active centre, but this interaction is worsened when the distance between that moiety and the ZBG of the compound is increased.

Regarding CA IX, this isozyme had the highest inhibitory activities observed, namely with compounds **1a**, **3a** and **4a**, displaying $K_I$ values of 2.1, 2.5 and 3.7 nM, respectively. In fact, all the sulfonamide-based compounds (**a**-type series) proved to be more active against CA IX than the reference inhibitors AAZ and SPESB, which have $K_I$ values of 25 and 18 nM, respectively. As it was found for CA II, the sulfonic derivatives (**b**-type series) are much less potent inhibitors of the isoform IX than their corresponding sulfonamide analogues, all of them presenting $K_I$ values larger than 1 μM, mainly because the sulfonate is a much less efficient ZBG than the sulfonamide.[14] In this case, the order of inhibitory activities of the sulfonamide-containing compounds is different from that of CA II, since the decreasing order for CA IX is **1a** > **3a** > **4a** > **2a**, while for CA II it is **1a** > **2a** > **4a** > **3a**. This fact must be intrinsically related to the differences in the structures of the two isozymes, and it may be determinant for a rational design of selective inhibitors. However, the difference in their activities towards CA IX is not as significant as for CA II; in fact the $K_I$ values are of the same order of magnitude, and thus not so dependent on the nature and length

of the spacer. The sulfonamide-based compounds, unlike the reference inhibitors AAZ and SPESB, also revealed more selective for CA IX with respect to the other tested CAs. With CA IX/CA II inhibition ratios ranging from 2.2 to 369, compound **3a** proved to be the most selective, whereas **1a**, in spite of being the most active inhibitor, was the less selective.

With regards to DHFR inhibition, the results showed greater variability in the potency of the synthesized antimetabolites towards this enzyme. Thus, compounds **2a** and **2b** did not affect the enzyme activity at concentrations up to 0.5 mM, while the other compounds demonstrated moderate inhibitory effects with the $IC_{50}$ values in the low micromolar range (from 1.3 to 20 μM). It has to be noted that methotrexate (MTX), a widely used anticancer drug, inhibits DHFR at low nanomolar concentrations ($IC_{50}$ is about 5 nM). Correspondingly, compounds **3b** and **4a**, which are structurally more similar to MTX, demonstrated the highest inhibitory activities ($IC_{50}$ values of 1.3 and 1.8 μM, respectively). On the other hand, the compounds with the simplest structures, **1a** and **1b**, have similar activities ($IC_{50}$ values of 2.5 and 2.0 μM, respectively). Interestingly, in these two compounds, the aromatic ring of the benzenesulfonyl moiety seems to occupy the same position as the aromatic ring of *p*ABA moiety of MTX, while the sulfonyl moiety is most probably positioned in the same region as the α-carboxyl group of the glutamate residue in MTX (see Fig. 1). The fact that the sulfonic analogue (compound **1b**) demonstrated slightly stronger inhibitory activity than the corresponding sulfonamide (compound **1a**) supports this suggestion. A similar trend was observed in case of compounds **3a** and **3b**, for which the difference in the $IC_{50}$ values is about 15-fold. In this case, however, the sulfonyl moiety should bind in other area, since the distance from this group to the pteridine moiety is significantly higher.

Summarizing, the presence of a benzene ring in the proximity of the 2,4-diamino-6-methylpteridine moiety is crucial for the binding and inhibiting DHFR, since even a slightly more remote position (difference in two methylene groups) yields inactive compounds (**2a** and **2b**).

### 3.2. Molecular modelling

#### 3.2.1. Docking of inhibitors to carbonic anhydrases (CAs)

In order to rationalize the inhibition results towards the CAs and DHFR with the new inhibitors, molecular modelling studies were carried out.

The compounds were docked into the crystal structures of CA II[15] and IX[16] (respectively, entries 1G54 and 3IAI of the RCSB Protein Data Bank),[17] using the GOLD software,[18] following a previously validated method.[13]

The docking result for the most active compound (**1a**) with CA IX is depicted in Figure 2. Analysis of this figure shows a major binding feature, common to all ligands, involving the benzenesulfonyl moiety, which is well accommodated in the active site of the CA, and coordinates the catalytic zinc ion by the anionic N-atom of the sulfonamide, while for the sulfonate the metal coordination involves the O-atom. In the case of the sulfonamides, two H-bonds are formed, one between its NH group and the hydroxyl group of Thr332 (numeration according to the hCA IX structure of UniProtKB database, entry Q16790);[19] another one between the SO group and the backbone NH of the same residue. In the case of the sulfonic analogues (such as **1b**, Fig. 2a), only one H-bond is formed, between the SO group oxygen and the backbone NH of Thr332. These differences explain the much lower inhibitory activities normally observed for the sulfonic analogues, as compared with the sulfonamides. In Figure 2a, it is also possible to verify that **1a** and **1b** bind in somewhat different manners, besides the similar interactions involving the ZBGs. The pteridine moiety of **1a** is well adjusted to the hydrophobic wall of the active cavity of CA IX and

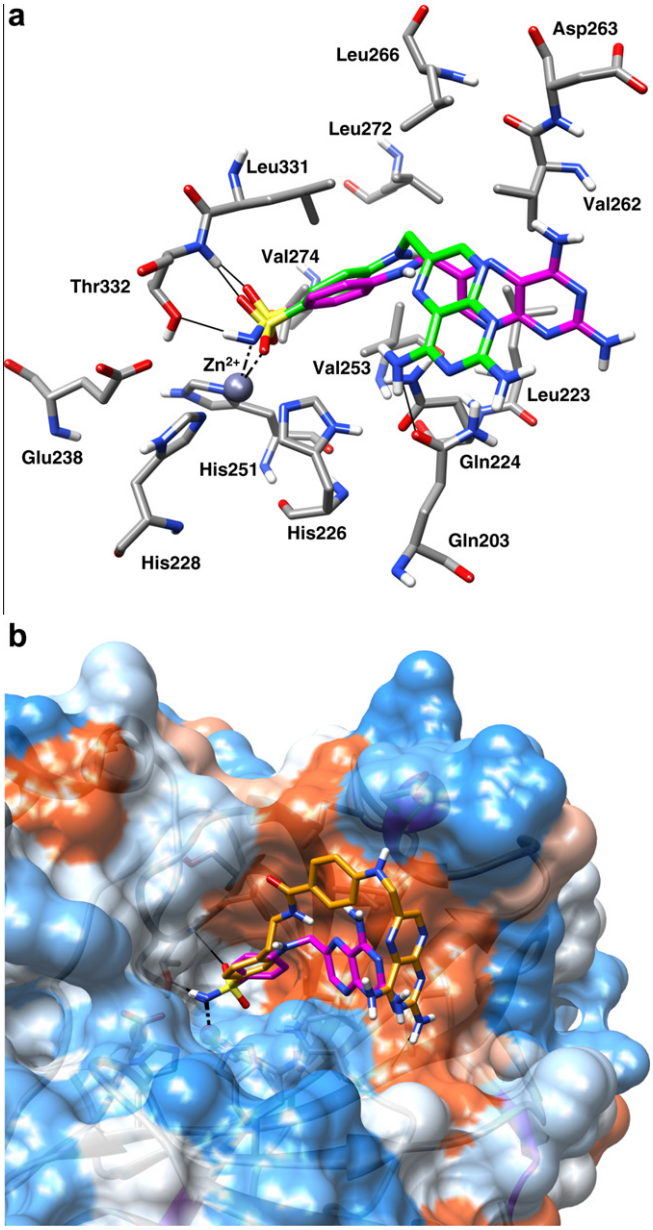


**Figure 2.** Docking of compounds into the CA IX active site: **1a** (magenta) superimposed with **1b** (light green) (a); **1a** (magenta) superimposed with **3a** (orange) (b). Red surfaces represent the hydrophobic and blue the hydrophilic regions of the protein; black dashed lines represent the ligand coordination to the metal, and the full lines represent the H-bonds formed with the protein.

establishes close contacts with the several valine and leucine residues forming that wall (namely Leu331, Leu266, Val262), which results in a good ligand–enzyme affinity. On the other hand, **1b** does not form so many hydrophobic interactions, but one of the $NH_2$ group forms an H-bond with the side-chain carbonyl group of Gln203. Furthermore, considering the proximity of the pteridine ring of compound **1a** towards the hydrophilic residue Gln224 (Fig. 2a), a slight flip of these groups may be expect, thus allowing a H-bonding between the side-chain $NH_2$ group and the aromatic nitrogen atoms of the pteridine, with a concomitant considerable increase of the adduct stability.

As regards compound **2a**, it binds with a conformation in between **1a** and **1b**, and therefore still preserves hydrophobic interaction with the protein, while establishes H-bonding with the $NH_2$ group of Gln224 (Fig. S1 of Supplementary data). Considering compounds **3a** and **4a**, their binding conformations are quite sim-

ilar to each other, but compared with **1a**, the longer spacers increased the distance between the pteridine ring and the benzenesulfonamide moiety, leading to a decrease of the hydrophobic interactions with the enzyme. On the other hand, the pteridine ring of **3a** may form an H-bond with the backbone carbonyl group of Leu223 (Fig. 2b). Moreover, it is noticeable the proximity of the carboxylic acid of Asp263 and the NH group of the *p*ABA moiety, for **3a**. Therefore, some H-bond interaction between these two groups may be also expected. This interplay of interactions may lead to complexes with similar stabilities, thus explaining the very close inhibitory activities of the different ligands (**1a**–**4a**) toward CA IX.

Analyzing the docking results with CA II, it was possible to confirm that the structural differences on the two proteins also lead to different binding modes of some ligands. In fact, compounds **1a** and **1b** were found to bind preferably the hydrophilic part of the cavity, forming a H-bond between the $NH_2$ group connected to the pteridine and the side-chain carbonyl of Asn67 (when referring to CA II, the residue numeration is according to the hCA II structure of UniProtKB, entry P00918), and therefore the hydrophobic interactions with the enzyme were reduced (see Fig. 3a). Compounds **2a**, **3a** and **4a** tend, in general, to be leaning over the hydrophobic part of the cavity, in a similar way to what happened with CA IX (see Fig. 3b). However, the interactions established are much weaker with CA II than with CA IX. The main reason for this difference is the type of hydrophobic residues forming this hydrophobic wall, which, in CA IX, is mostly based on leucine and valine residues. Thus, the substitution of Leu266 in CA IX for the smaller Val134 in CA II, and, respectively, of Val262 for Phe130, decreases the number of hydrophobic interactions established with CA II. On the other hand, while on CA IX the Asp263 residue may, in certain cases, form hydrophilic interactions with our inhibitors (such as for

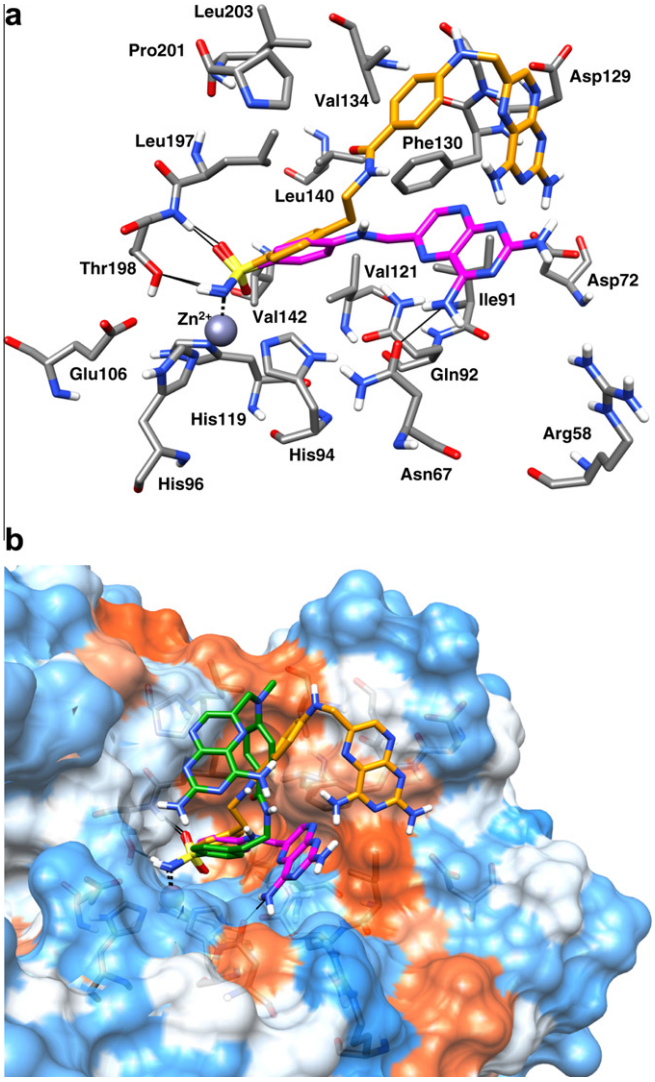


**Figure 3.** Docking of compounds into the CA II active site: **1a** (magenta) superimposed with **3a** (orange) (a); **1a** (magenta) superimposed with **3a** (orange) and **4a** (green) (b). Red surfaces represent the hydrophobic and blue the hydrophilic regions of the protein; black dashed lines represent the ligand coordination to the metal, and the full lines represent the H-bonds formed with the protein.

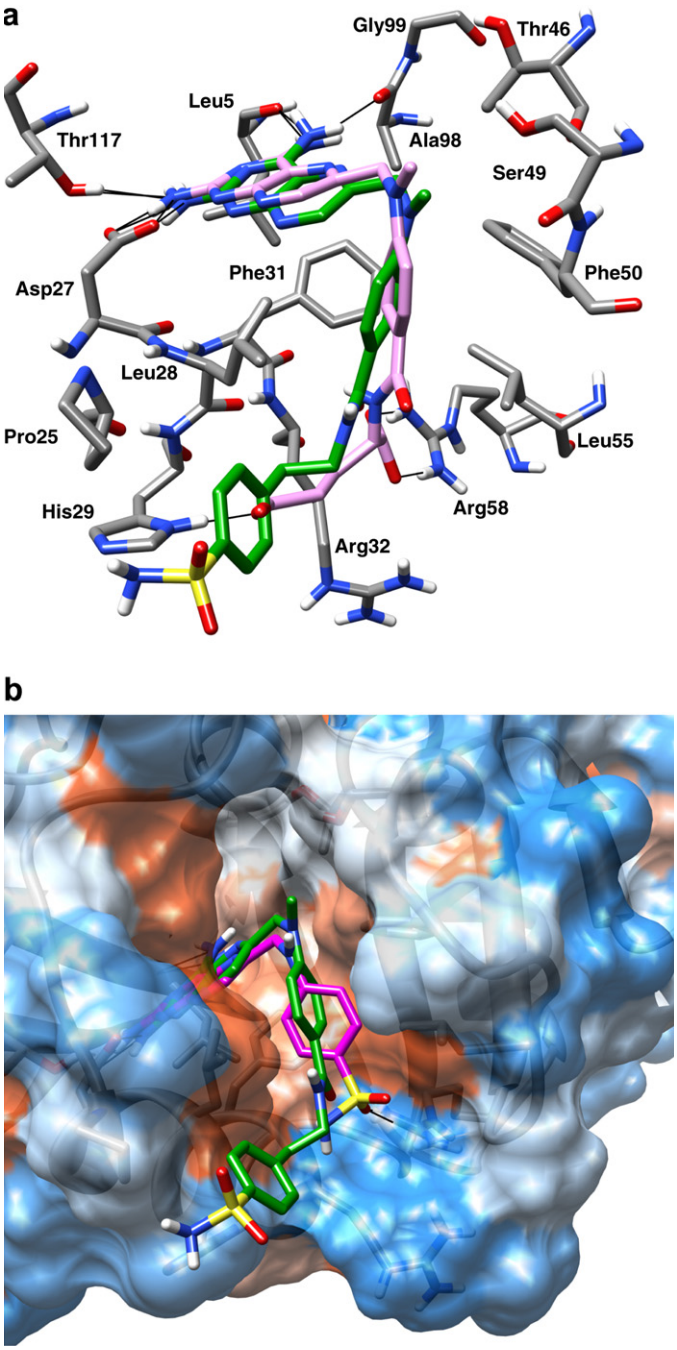


**Figure 4.** Docking of compounds to DHFR: MTX (pink) superimposed with **4a** (green) (a); **4a** (green) superimposed with **1a** (magenta) (b). Red surfaces represent the hydrophobic and blue the hydrophilic regions of the protein; the full black lines represent the H-bonds formed between the ligand and the protein.

**3a**), on CA II it is substituted by Gly131, and so this type of interactions is no longer possible (see Supplementary data, Fig. S2).

Altogether, these features seem to explain the activity and selectivity profiles displayed by these compounds towards CA II and IX, which proved to be in general more selective for inhibiting CA IX than the isozyme II. Furthermore, the suggested differences between the structures of these two enzymes may be used in the future for the rational design of more active and CA IX-selective inhibitors of this type.

### 3.2.2. Docking of inhibitors to DHFR

The target compounds were also docked into a crystal structure of *L. casei* DHFR, originally complexed with MTX[20] (PDB entry 3DFR). The results showed that for all the compounds, the pteridine moiety is able to have a good accommodation into the cavity of the DHFR active centre, and is positioned in a very similar way as MTX. The interactions between that group within the hydrophobic pocket of the enzyme may be established in the same way, namely the π–π contact with the residue Phe31 (numeration according to entry P00381 of UniProtKP database) and H-bonds between the $NH_2$ groups and the carboxylate of Asp27, the hydroxyl of Thr117, and the backbone carbonyls of Leu5 and Ala98 (see Fig. 4a). Considering the most active inhibitors (compounds of types **1**, **3**, and **4**), they all contain an aromatic group directly bound to the pteridine moiety, as the *p*ABA group in the case of MTX. Moreover, the docking studies demonstrated that this group is placed in a similar way as that of MTX, as was suggested before by our SAR analysis. This feature results in the same strong hydrophobic interactions, namely with the residues Phe31, Leu28, Phe50, and Leu55. In fact, the lack of this *p*ABA moiety in compounds **2a** and **2b** (which have a $CH_2CH_2$ group in its place, see Fig. S3 in Supplementary data) results in the very poor inhibitory activity displayed by these compounds, thus revealing how important this feature is for a good interaction with DHFR. Concerning compounds **3a**, **3b** and **4a**, they all bind in a similar manner, namely the benzenesulfonyl moiety lying over the same hydrophobic valley as MTX (see Fig. 4b and Fig. S4 of Supplementary data). However, while this inhibitor forms strong H-bonds between the α-carboxylate and the guanidinium group of Arg58, and the γ-carboxylate with the side-chain NH of His29, our inhibitors form only weak hydrophobic interactions with the residues forming this valley (namely Leu28 and Pro25), and this fact accounts for their ca. 1000-fold weaker inhibitory activity. The docking calculations also demonstrated that the pteridine and *p*ABA groups form the same interactions in these three families of compounds (**1**, **3** and **4**). Since compounds **1a** and **1b** presented $IC_{50}$ values close to inhibitors of type **3** and **4**, the possibility of the sulfonyl group in family **1** to form a H-bond with Arg58 (as MTX) probably overcomes the larger number of hydrophobic interactions established in families **3** and **4**, thus resulting in similar inhibitory activities (Fig. 4b).

### 3.3. Antiproliferative effect

Antiproliferative effects of the synthesized compounds were evaluated on two cancer cell lines: non-small cell lung carcinoma (A549) and prostate carcinoma (PC3). Effects of the compounds were compared to antiproliferative effects of MTX as a control. Cell viability was assessed using MTT cell proliferation assay, as previously described.[21] These assays demonstrated (see Table 1) that PC3 cells, in general, are more sensitive to the inhibition by both MTX ($IC_{50}$ is fivefold lower) and by the synthesized compounds ($IC_{50}$ are 2–10-fold lower). However, despite the fact that most of the synthesised compounds inhibited both DHFR and CAs at low micromolar and low nanomolar concentrations, respectively, effects on cell proliferation were noted only at low millimolar concentrations for both cell lines. This suggests that, most likely, the compounds were not transported across the cell membrane. While CA IX was shown to be a membrane isoform with the active site extracellularly exposed,[8] that could be affected by the inhibitors in the medium, DHFR, as well as CA I and II, are strictly intracellular-located proteins, and for their inhibition the compounds should be transported inside the cells. Apparent absence of the effect of CA IX inhibition on cell grows in culture can be explained by the fact that both CA IX and XII grant the survival advantage to hypoxic tumor cells by regulating and maintaining pH.[10] In our cell culture models, cells grew in monolayer and have never become hypoxic. So, inhibition of the mechanism that helps survive hypoxic conditions had no effect in cell culture. Tumor xenograft model would be more useful to evaluate the effect of this CA inhibition on tumor cell survival.

## 4. Conclusions

New bifunctional compounds based on the conjugation of the aminopteridine and arylsulfonamide pharmacophores have been developed for the blockage of two unrelated pathways involved in cancer development and proliferation, which are dependent on the enzymatic activity of DHFR and CA IX. In particular, after the design and preparation of the dual targeting compounds, their inhibitory activities were evaluated towards a set of CAs (CA I, II and IX), DHFR, and their antiproliferative effects were tested in two cancer cell lines (A549 and PC-3). As for the CA inhibition, some compounds presented low nanomolar activity, with compound **1a** displaying the lowest $IC_{50}$ value (2.1 nM) over CA IX, and selectivity for the cancer-related CA IX over the ubiquitous CA II rising up to 369 for compound **3a**. In terms of DHFR inhibition, most of the compounds presented activities in the low micromolar range, namely with 2.5 μM for **1a** and 1.3 μM for **3b**. The antiproliferative properties of the new compounds against the two cell lines were more disappointing, with activities in the millimolar concentration range, probably due to deficiency of the inhibitor transport inside the cells. In general, the inhibitory profiles towards the CAs and DHFR revealed good antitumor potential of these new bifunctional compounds, but apparently better cell permeability properties would be required to improve their efficacy. Thus, further development of this type of compounds, based on a rational molecular design including physicochemical and pharmacokinetic considerations, could be of great interest in finding new effective multi-target anticancer agents.

## 5. Experimental part

### 5.1. General methods

All the commercially available reagents were of the highest purity and were used without further purifications. Folic acid, methotrexate, *O*-benzotriazol-1-yl-*N*,*N*,*N*′,*N*′-tetramethyluronium-tetrafluoroborate (TBTU), *N*-methylmorpholine (redistilled), $NH_2OH$, thionylbromide, di-*tert*-butyl dicarbonate, sulfanilic acid, 4-(2-aminoethyl)-benzenosulfonamide were purchased from *Sigma–Aldrich*, and 4-aminobenzoic acid, 4-(methylamino)benzoic acid, 2,4-diamino-6-(hydroxylmethyl)pteridine hydrochloride, sulfanilamide from *Acros Organics*. The solvents were purchased from *Acros Organics* or *Merck* and, whenever necessary, they were purified and dried according to standards methods.[22] All moisture-sensitive reactions were performed under nitrogen atmosphere. The chemical reactions were followed by TLC using silica gel plates (G-60 $F_{254}$, Merck). A Bio-Rad Merlin, FTS 3000 MX spectrometer was used to record solid state IR spectra (KBr pellets). $^1H$ and $^{13}C$ NMR spectra were recorded on a Varian Unity 300 FT NMR spectrometer at 25 °C. When necessary, assignment of the signals of the $^{13}C$ NMR signals were confirmed by DEPT. Chemical shifts are

reported in ppm ($\delta$) with tetramethylsilane (TMS) as internal reference, in organic solvents and sodium 3-(trimethylsilyl)-[2,2,3,3-$D_4$]-propionate (DSS) in $D_2O$ solutions. The following abbreviations are used: s = singlet; d = doublet; t = triplet; m = multiplet; br = broad. Mass spectra (FAB) were performed in a VG TRIO-2000 GC/MS instrument, and the ESI mass spectra on a 500 MS LC Ion Trap (Varian Inc., Palo Alto, CA, USA) mass spectrometer equipped with an ESI ion source, operated either in positive or negative ion modes. Elemental analyses were performed on a Fisons EA 1108 CHNF/O instrument.

### 5.2. Synthesis of the compounds

#### 5.2.1. 6-(Bromomethyl)pteridine-2,4-diamine (PtBr)

2,4-Diamino-6-(hydroxymethyl)-pteridine (PtOH, 0.5 g, 2.60 mmol) was dissolved in thionyl bromide (10 mL) and the reaction mixture was stirred for 24 h at rt. Thionyl bromide was evaporated in vacuum and the solid residue was washed with large amount of dry toluene (ca. 100 mL), affording the product as brown crystals (0.623 g, 94% yield); mp 168–170 °C. $^1$H NMR (300 MHz, DMSO-$d_6$) $\delta$: 9.04 (1H, s, C*H*(Pt)), 8.60 and 7.97 (2H each, s, N$H_2$(Pt)), 4.89 (2H, s, C$H_2$(Pt)); $^{13}$C NMR (DEPT) (300 MHz, DMSO-$d_6$) $\delta$: 149 (*C*H(Pt)), 30.9 (*C*H$_2$(Pt)); IR (KBr, cm$^{-1}$): 578, 523, 721, 611 ($\nu_{C\text{-}Br}$); MS (FAB) *m/z*: 255, 257 (M+1, M+3) (twin peaks).

#### 5.2.2. 4-((2,4-Diaminopteridin-6-yl)methylamino) benzenesulfonamide (1a)

General procedure for preparation of the target compounds (for **1a**–**4a** and **1b**–**3b**), from PtBr: a mixture of sulfanilamide (0.200 g, 1.16 mmol) and NaH (80% in paraffin oil, 0.035 g, 1.16 mmol) in dry DMF (15 mL) was stirred for 40 min. Then PtBr (0.295 g, 1.16 mmol) and $CaCO_3$ (0.058 g, 0.58 mmol) were added, and the mixture was stirred under nitrogen, in the dark at rt for a week. The solvent was then evaporated under high vacuum. The solid residue was taken into water and a yellow solid precipitated, which was then filtered and washed with ethanol and diethyl ether. Recrystallization from DMF afforded the pure compound as yellow crystals (0.370 g, 92% yield). Mp 265–266 °C; $^1$H NMR (300 MHz, DMSO-$d_6$) $\delta$: 9.09 and 9.12 (2H each, s, N$H_2$(Pt)), 8.82 (1H, s, C*H*(Pt)), 7.66 (2H, d, C*H*=C–S), 7.06 (1H, t, N*H*), 6.98 (2H, s, SO$_2$N$H_2$), 6.79 (2H, d, NH–C=C*H*), 4.60 (2H, s, C$H_2$(Pt)); IR (KBr, cm$^{-1}$): 3356, 3154 ($\nu_{NH}$), 1151, 1315 ($\nu_{SO2NH2}$), 569, 545 ($\nu_{SN}$), 831 ($\nu_{NH,\ aromatic}$); MS (ESI) *m/z*: 347.1 (M+H)$^+$.

#### 5.2.3. 4-((2,4-Diaminopteridin-6-yl)methylamino) benzenesulfonic acid (1b)

From PtBr and sulfanilic acid, as in the case of **1a**. Yellow crystals (34%), mp higher than 300 °C. $^1$H NMR (300 MHz, DMSO-$d_6$) $\delta$: 9.08 and 8.90 (2H each, s, N$H_2$(Pt)), 8.82 (1H, s, C*H*(Pt)), 7.56 (2H, d, C*H*=C–S), 6.98 (1H, s, SO$_3$*H*), 6.81 (2H, d, NH–C=C*H*), 6.76 (1H, t, N*H*), 4.61 (2H, s, C$H_2$(Pt)); MS (ESI) *m/z*: 348.1 (M+H)$^+$.

#### 5.2.4. 4-(2-((2,4-Diaminopteridin-6-yl)methylamino)ethyl) benzenesulfonamide (2a)

From PtBr and (4-(2-aminoethyl)-benzenesulfonamide (AEBS), as in the case of **1a**. Yellow crystals (14%); mp higher than 300 °C; $^1$H NMR (300 MHz, DMSO-$d_6$) $\delta$: 8.63 (1H, s, C*H*(Pt)), 7.73 and 7.48 (2H each, s, N$H_2$(Pt)), 7.63 (2H, d, C*H*=C–S), 7.32 (2H, d, CH$_2$–C=C*H*), 6.57 (1H, m, N*H*), 4.13 (2H, s, SO$_2$N$H_2$), 3.92 (2H, s, C$H_2$(Pt)), 2.89 (2H, t, NH–C$H_2$), 2.73 (2H, t, C$H_2$–C=CH); IR (KBr, cm$^{-1}$): 3356 ($\nu_{NH}$), 1159 ($\nu_{SO2NH2}$), 707 ($\nu_{SN}$), 875 ($\nu_{NH,aliphatic}$); MS (ESI) *m/z*: 375.2 (M+H)$^+$, 397.1 (M+Na)$^+$.

#### 5.2.5. 4-(2-Aminoethyl)benzenesulfonic acid

To a solution of AEBS (0.50 g, 2.5 mmol) in a mixture of THF (5 mL) and 2 M HCl solution (10 mL) was added $NaNO_2$ (0.30 g, 4.25 mmol), and the mixture was stirred at 40 °C for 24 h. After evaporation of the organic solvent, the resulting solution was taken into $CH_3CN$ (10 mL), and the white precipitate was filtered and dried. Recrystallization with dry methanol allowed removal of the inorganic material, affording the pure hydrochloric salt of the title compound as white crystals (0.416 g, 70% yield); mp higher than 320 °C; $^1$H NMR (300 MHz, $D_2O$) $\delta$: 7.76 (2H, d, C*H*=C–S), 7.42 (2H, d, CH$_2$–C=C*H*), 3.29 (2H, t, NH–C$H_2$), 3.04 (2H, t, C$H_2$–C=CH); IR (KBr, cm$^{-1}$): 3134, 3078 ($\nu_{SO3H}$); MS (FAB) *m/z*: 202 (M+H)$^+$.

#### 5.2.6. 4-(2-((2,4-Diaminopteridin-6-yl)methylamino)ethyl) benzenesulfonic acid (2b)

From PtBr and 4-(2-aminoethyl)benzenesulfonic acid, as in the case of **1a**, but using 3 equiv of NaH. Yellow crystals (40%), mp higher than 300 °C; $^1$H NMR (300 MHz, DMSO-$d_6$) $\delta$: 8.63 (1H, s, C*H*(Pt)), 7.58 (2H, d, C*H*=C–S), 7.22 (2H, d, CH$_2$–C=C*H*), 6.99 (1H, m, N*H*), 5.01 (1H, s, SO$_3$*H*), 3.94 (2H, s, C$H_2$(Pt)), 2.75 (2H, t, NH–C$H_2$), 2.58 (2H, t, C$H_2$–C=CH); MS (ESI) *m/z*: 398.1 (M+Na)$^+$.

#### 5.2.7. 4-(*tert*-Butoxycarbonylamino)benzoic acid (5)

A solution of 4-aminobenzoic acid (*p*ABA, 1.03 g, 7.5 mmol) in water (8 mL) and 1,4-dioxane (8 mL) was cooled in an ice bath at 0 °C, followed by the parallel addition of $Na_2CO_3$ (1.53 g, 15 mmol) in water (10 mL) and di-*tert*-butyl-dicarbonate (*Boc*$_2$O, 1.80 g, 8.25 mmol) in 1,4-dioxane (10 mL). The reaction mixture was stirred for 4 h at 0 °C and then it was left at rt overnight. The pH of the solution was lowered up to 2 with 2 M HCl and the product precipitated as a white solid, which was filtered and washed with large amount of HCl solution to give the pure product as white crystals (1.69 g, 95% yield); mp 205–206 °C; $^1$H NMR (300 MHz, acetone-$d_6$) $\delta$: 7.85 (2H, d, C*H*=C–CO), 7.39 (2H, d, NH–C=C*H*), 1.51 (9H, s, C(C$H_3$)$_3$); IR (KBr, cm$^{-1}$): 3390, 3423, 3484, 3566 ($\nu_{NH}$); MS (ESI) *m/z*: 236.4 (M−H)$^-$.

#### 5.2.8. *tert*-Butyl 4-(4-sulfamoylphenethylcarbamoyl) phenylcarbamate (6a)

To an ice-cooled solution of *N*-methylmorpholine (0.23 mL, 2.10 mmol) and **5** (0.25 g, 1.05 mmol) in dry DMF (10 mL) under nitrogen was added TBTU (0.34 g, 1.05 mmol), and the mixture was stirred for 50 min. A solution of AEBS (0.21 g, 1.05 mmol) in dry DMF (5 mL) was then added and resulting solution was left stirring for 5 h at 0 °C, and, then, it was left to heat up to rt and was stirred overnight. The solvent was evaporated under high vacuum and the solid residue was taken into large amount of water (50 mL), and then a pale yellow solid was precipitated, which was filtered, washed with methanol (40 mL), and dried under vacuum, affording the pure product as white crystals (0.198 g, 45% yield); mp 255–258 °C; $^1$H NMR (300 MHz, MeOD) $\delta$: 7.72 (2H, d, C*H*=C–S), 7.58 (2H, d, C*H*=C–CO), 7.37 (2H, d, NH–C=C*H*), 7.31 (2H, d, CH$_2$–C=C*H*), 3.50 (2H, t, NH–C$H_2$), 2.88 (2H, t, C$H_2$–C=CH), 1.41 (9H, s, C(C$H_3$)$_3$); MS (ESI) *m/z*: 442.1 (M+Na)$^+$.

#### 5.2.9. 4-Amino-*N*-(4-sulfamoylphenethyl)benzamide (7a)

Removal of the *Boc* protecting group was performed by stirring a solution of **6a** (0.15 g, 0.36 mmol) in trifluoroacetic acid (TFA, 1 mL) and $CH_2Cl_2$ (1 mL) at rt for 5 h. After evaporation of the solvent, recrystallization from dry methanol/diethyl ether afforded the pure product as white crystals (0.062 g, 54% yield); mp 243–245 °C; $^1$H NMR (300 MHz, MeOD) $\delta$: 7.73 (2H, d, C*H*=C–S), 7.45 (2H, d, C*H*=C–CO), 7.35 (2H, d, CH$_2$–C=C*H*), 6.65 (2H, d, NH$_2$–C=C*H*), 3.50 (2H, t, NH–C$H_2$), 2.90 (2H, t, C$H_2$–C=CH); $^{13}$C NMR (DEPT) (300 MHz, DMSO-$d_6$) $\delta$:134 (*C*H=C–CO), 132 (CH$_2$–C=*C*H),

130 (*C*H=C–S), 43.8 (NH–*C*$H_2$), 120 ($NH_2$–C=*C*H), 40.1 (*C*$H_2$–C=CH); IR (KBr, $cm^{-1}$): 3328, 3210 ($\nu_{NH}$), 1190, 1342 $cm^{-1}$ ($\nu_{SO2NH2}$), 593, 545 ($\nu_{SN}$), 1726 ($\nu_{CO}$); MS (FAB) *m/z*: 320 $(M+H)^+$.

#### 5.2.10. 4-((2,4-Diaminopteridin-6-yl)methylamino)-*N*-(4-sulfamoylphenethyl)benzamide (3a)

From PtBr and **7a**, as in the case of **1a**. Yellow crystals (83%); mp 280–281 °C; $^1$H NMR (300 MHz, DMSO-$d_6$) $\delta$: 8.71 (1H, s, C*H*(Pt)), 8.20 (1H, t, CON*H*), 7.97 and 7.85 (2H each, s, N$H_2$(Pt)), 7.75 (2H, d, C*H*=C–S), 7.65 (2H, d, C*H*=C–CO), 7.42 (2H, d, $CH_2$–C=C*H*), 6.74 (2H, d, NH–C=C*H*), 6.63 (1H, m, N*H*), 4.50 (2H, s, C$H_2$(Pt)), 4.13 (2H, s, $SO_2NH_2$), 3.19 (2H, t, NH–C$H_2$), 2.91 (2H, t, C$H_2$–C=CH); IR (KBr, $cm^{-1}$): 3351, 3220 ($\nu_{NH}$), 1191, 1327 ($\nu_{SO2NH2}$), 590, 550 ($\nu_{SN}$), 875 ($\nu_{NH,aliphatic}$); MS (ESI) *m/z*: 494.2 $(M+H)^+$.

#### 5.2.11. 4-(2-(4-(*tert*-Butoxycarbonylamino)benzamido) ethyl) benzenesulfonic acid (6b)

From **5** and 4-(2-aminoethyl)benzenesulfonic acid, as in the case of **6a**. White crystals (32%); mp 200 °C (decomposition); $^1$H NMR (300 MHz, $D_2O$) $\delta$: 7.70 (2H, d, C*H*=C–S), 7.54 (2H, d, C*H*=C–CO), 7.37 (4H, m, NH–C=C*H*, $CH_2$–C=C*H*), 3.61 (2H, t, NH–C$H_2$), 2.95 (2H, t, C$H_2$–C=CH), 1.47 (9H, s, C($CH_3$)$_3$); MS (ESI) *m/z*: 419.1 $(M-H)^-$.

#### 5.2.12. 4-(2-(4-Aminobenzamido)ethyl)benzenesulfonic acid (7b)

From **6b,** by removal of the protecting group, as in the case of **7a**. White crystals (70%); mp 280–290 °C (decomposition); $^1$H NMR (300 MHz, $D_2O$) $\delta$: 7.70 (2H, d, C*H*=C–S), 7.57 (2H, d, C*H*=C–CO), 7.38 (2H, d, $CH_2$–C=C*H*), 7.17 (2H, d, NH–C=C*H*), 3.65 (2H, t, NH–C$H_2$), 2.98 (2H, t, C$H_2$–C=CH); IR (KBr, $cm^{-1}$): 3325, 3073 ($\nu_{SO3H}$); MS (ESI) *m/z*: 321.1 $(M+H)^+$.

#### 5.2.13. 4-(2-(4-((2,4-Diaminopteridin-6-yl)methylamino) benzamido)ethyl) benzenesulfonic acid (3b)

From PtBr and **7b**, as in the case of **1a**. Yellow crystals (95%); mp higher than 300 °C; $^1$H NMR (300 MHz, DMSO-$d_6$) $\delta$: 8.76 (1H, s, C*H*(Pt)), 8.15 (1H, t, CON*H*), 7.62 (2H, d, C*H*=C–S), 7.49 (2H, d, C*H*=C–CO), 7.14 (2H, d, $CH_2$–C=C*H*), 6.80 (1H, m, N*H*), 6.70 (2H, d, NH–C=C*H*), 5.07 (1H, s, $SO_3H$), 4.54 (2H, s, C$H_2$(Pt)), 2.78 (4H, m, NH–C$H_2$, C$H_2$–C=CH); IR (KBr, $cm^{-1}$): 3325, 3073 ($\nu_{SO3H}$), 1647 ($\nu_{CO}$); MS (ESI) *m/z*: 493.1 $(M-H)^-$.

#### 5.2.14. 4-(Methylamino)-*N*-(4-sulfamoylphenethyl)benzamide (8)

From 4-(methylamino)benzoic acid (NMe*p*ABA) and AEBS, as in the case of **6a**. White crystals (82%); mp 264–267 °C; $^1$H NMR (300 MHz, DMSO-$d_6$) $\delta$: 8.24 (1H, t, CON*H*), 7.80 (2H, d, C*H*=C–S), 7.68 (2H, d, C*H*=C–CO), 7.47 (2H, d, $CH_2$–C=C*H*), 7.34 (1H, m, N*H*$CH_3$), 6.70 (2H, d, NH–C=C*H*), 6.25 (2H, s, $SO_2NH_2$), 3.49 (2H, t, NH–C$H_2$), 2.85 (2H, t, C$H_2$–C=CH), 2.76 (3H, s, NC$H_3$); $^{13}$C NMR (DEPT) (300 MHz, DMSO-$d_6$) $\delta$: 134 (*C*H=C–CO, $CH_2$–C=*C*H), 131 (*C*H=C–S), 115 (NH–C=*C*H), 44.4 (NH–*C*$H_2$), 40.2 (*C*$H_2$–C=CH), 34.5 (N*C*$H_3$); IR (KBr, $cm^{-1}$): 3411, 3351, 3315 ($\nu_{NH}$), 1334, 1311, 1164 ($\nu_{SO2NH2}$), 740, 690, 543, 590 ($\nu_{SN}$), 1524 ($\nu_{CO}$); MS (FAB) *m/z*: 334 $(M+H)^+$.

#### 5.2.15. 4-((2,4-Diaminopteridin-6-yl)methyl)(methyl)amino)-*N*-(4-sulfamoylphenethyl)-benzamide (4a)

From PtBr and **8**, as in the case of **1a**. Yellow crystals (75%); mp 245–250 °C; $^1$H NMR (300 MHz, DMSO-$d_6$) $\delta$: 8.63 (1H, s, C*H*(Pt)), 8.23 (1H, t, CON*H*), 7.72 (2H, d, C*H*=C–S), 7.65 (2H, d, C*H*=C–CO), 7.40 (2H, d, $CH_2$–C=C*H*), 7.28 (2H, s, N$H_2$), 6.79 (2H, d, NH–C=C*H*), 4.81 (2H, s, C$H_2$(Pt)), 4.38 (2H, s, $SO_2NH_2$), 3.44 (2H, t, NH–C$H_2$), 3.24 (3H, s, NC$H_3$), 2.89 (2H, t, C$H_2$–C=CH); IR (KBr, $cm^{-1}$): 3355, 3220 ($\nu_{NH}$), 1330, 1317 ($\nu_{SO2NH2}$), 598, 548, 650 ($\nu_{SN}$); MS (ESI) *m/z*: 508.2 $(M+H)^+$.

### 5.3. CA inhibition assays

Recombinant human CA isoforms I, II and IX have been prepared as reported earlier by our group,[23,24] and their activity assayed by a stopped flow $CO_2$ hydration assay.[25] An Applied Photophysics (Oxford, UK) stopped-flow instrument has been used for assaying the CA-catalyzed $CO_2$ hydration activity. A phenol red solution (0.2 mM) was used as indicator, working at the absorbance maximum of 557 nm, with 10 mM Hepes (pH 7.5) as buffer, 0.1 M $Na_2SO_4$ (for maintaining constant the ionic strength), following the CA-catalyzed $CO_2$ hydration reaction for a period of 10–100 s. The $CO_2$ concentrations ranged from 1.7 to 17 mM for the determination of the kinetic parameters and inhibition constants. For each inhibitor at least six traces of the initial 5–10% of the reaction have been used for determining the initial velocity. The uncatalyzed rates were determined in the same manner and subtracted from the total observed rates. Stock solutions of inhibitor (1 mM) were prepared in distilled–deionized water with 10–20% (v/v) DMSO (which is not inhibitory at these concentrations) and dilutions up to 0.1 nM were done thereafter with distilled–deionized water. Inhibitor and enzyme solutions were preincubated together for 15 min at room temperature prior to assay, in order to allow for the formation of the E–I complex. The inhibition constants were obtained by non-linear least-squares methods using PRISM 3, from Lineweaver–Burk plots, as reported earlier, and represent the average from at least three different determinations.[23,24]

### 5.4. DHFR inhibition assays

DHFR activity (the enzyme from *L. Casei* was used), in the presence and in the absence of inhibitors, has been assayed spectrophotometrically by monitoring the decrease in absorbance at 340 nm due to oxidation of NADPH. All assays were performed at 30 °C in a Shimadzu 2401PC double-beam spectrophotometer. The reaction mixture contained 100 μM of dihydro-folic acid, 150 μM of NADPH and 2.5 μg/mL purified DHFR. The reaction was started by the addition of the enzyme (1–2.5 μg) in a final volume of 1.0 mL and read against a blank cuvette containing all components except the enzyme. Synthesized compounds were added in the reaction mixture to final concentrations 0.1–1000 μM. For a reference inhibition curve, MTX was added into reaction mixture to final concentrations of 0.001–0.1 μM.

### 5.5. Cell culture assays

The lung carcinoma cell line A549 was obtained from American Type Culture Collection. The prostate carcinoma cell line PC3 was a kind gift from Dr. James Norris, Medical University of South Carolina. Cells were maintained in RPMI-1640 supplemented with 10% heat-inactivated fetal bovine serum, 2 mM glutamine and 1 mM sodium pyruvate (complete medium). All cells were grown at 37 °C under humidified air containing 5% $CO_2$. Cells were plated in 96-well plates at a density of about 5000 cell/well. Treatment with different concentrations of a corresponding inhibitor was performed constantly for 72 h. MTT cell proliferation assay was performed using CellTiter 96 kit (Promega) according to manufacturer's directions.

### 5.6. Molecular modelling

#### 5.6.1. Docking of ligands with CA II and CA IX

The X-ray structures of hCA II and IX complexed with inhibitors were taken from the RCSB Protein Data Bank (entries 1G54 and

3IAI, respectively).[17] With the purpose of further result comparison, these structures were aligned, using UCSF Chimera software.[26] The crystal structures were then treated with Maestro 7.5,[27] and all counterions, co-crystallization ligands and solvent molecules were removed. The hydrogen atoms were added using the all-atom model, the ligands were extracted from the complex structure and then saved in different files to be further used for defining the binding site in the docking calculations. The structures of our inhibitors were built using Maestro 7.5, and were minimized by means of Macromodel.[28] The conjugated gradient method was applied, until a convergence value of 0.05 kJ/Å mol was reached, using the MMFFs force field and a water environment model (generalized-Born/surface-area model), with a distance-dependent dielectric constant of 1.0. The minimized ligands were then subjected to a conformational search (CS) of 100 steps, in which an algorithm based on the Monte Carlo method was used, with the same force field and parameters as in the minimization.

The minimized ligands were docked into the two CA structures with the GOLD program,[18] version 4.0, following a previously validated procedure for docking and virtual screening of ligands with CAs.[13] The region of interest used by Gold was defined in order to contain the residues within 15 Å from the position of the original ligands in the X-ray structures. The 'allow early termination' option was deactivated, while the possibility for the ligand to flip ring corners was activated. The zinc ion was set with a tetrahedral coordination, and the three water residues were allowed for spinning during the docking, in order to find better hydrogen orientation. The remaining Gold default parameters were used, and the ligands were submitted to 200 genetic algorithm (GA) runs. The ChemScore fitness function was used, and two protein H-bond constraints were imposed, one between the hydroxyl O-atom and another with the NH H-atom of Thr198 residue (hCAII numeration), and the ligands.

### 5.6.2. Docking of ligands with DHFR

To validate the best docking procedure using Gold software, seven crystal structures of DHFR complexes were taken from the RCSB Protein Data Bank (entries 3DFR, 1U72, 2W3M, 2W3B, 3GHW, 2W3A, and 1BOZ), and these structures were treated with Maestro 7.5, as described above for the CAs, removing all solvent, ions and NADPH molecules when they were present. The respective ligands in each complex structure were energy-minimized by means of Macromodel, as described before for the ligands. The resulting structures were then docked into the respective protein structures with Gold. In each case, the binding site was defined as the atoms within 15 Å from the original position of the respective ligand. The 'allow early termination' option was deactivated, while the possibility for the ligand to flip ring corners was activated. All the remaining Gold default parameters were used with no further constraints, and the ligands were submitted to 100 GA steps runs, using the three scoring functions supplied by Gold: ASP, ChemScore and GoldScore. The best ranked solution in each case was compared with the original conformation in the respective X-ray structure, and the rmsd (root mean square deviation) was calculated for the heavy atoms. From the three fitness functions tested, ASP gave the best docking results (average rmsd for the seven docking results of 0.83 Å), and it was further used to dock our ligands, following the same procedure. For this purpose, the DHFR structure from the PDB complex 3DFR was used.

## Acknowledgements

The authors would like to thank the portuguese Fundação para a Ciência e Tecnologia for the post-doc Grants SFRH/BPD/11653/2002 (E. Enyedy) and SFRH/BPD/29874/2006 (S. Marques). We also thank the Portuguese NMR and MS networks (IST-UTL Center), created by the Portuguese Foundation for Science and Technology (FCT), for providing access to their facilities. This research was also financed in part by an EU grant of the 7th Fp (Metoxia projecy) to C.T. Supuran.

All molecular modeling figures and alignments of the enzyme structures were produced using the UCSF Chimera package, from the Resource for Biocomputing, Visualization, and Informatics at the University of California, San Francisco (supported by NIH Grant P41 RR-01081).

## Supplementary data

Supplementary data associated with this article can be found, in the online version, at doi:10.1016/j.bmc.2010.05.072.

## References and notes

1. Morphy, R.; Rankovic, Z. *J. Med. Chem.* **2005**, *48*, 6523.
2. Zimmermann, G. R.; Lehár, J.; Keith, C. T. *Drug Discovery Today* **2007**, *12*, 34.
3. Santos, M. A.; Enyedy, É. A.; Rossello, A.; Carelli, P.; Krupenko, N. I.; Krupenko, S. A. *Bioorg. Med. Chem.* **2007**, *15*, 1266.
4. Marques, S. M.; Nuti, E.; Rossello, A.; Supuran, C. T.; Tuccinardi, T.; Martinelli, A.; Santos, M. A. *J. Med. Chem.* **2008**, *51*, 7968.
5. Curtin, N. J.; Hughes, A. N. *Lancet Oncol.* **2001**, *2*, 298.
6. Gangjee, A.; Jain, H. D.; Phan, J.; Lin, X.; Song, X.; McGuire, J. J.; Kisliuk, R. L. *J. Med. Chem.* **2006**, *49*, 1055.
7. Pastorek, J.; Pastoreková, S.; Callebaut, I.; Mornon, J. P.; Zelník, V.; Opavský, R.; Zat'ovicová, M.; Liao, S.; Portetelle, D.; Stanbridge, E. J.; Zavada, J.; Burny, A.; Kettmann, R. *Oncogene* **1994**, *9*, 2877.
8. Thiry, A.; Dogné, J.-M.; Masereel, B.; Supuran, C. T. *Trends Pharmacol. Sci.* **2006**, *27*, 566.
9. Svastova, E.; Hulíková, A.; Rafajová, M.; Zat'ovičová, M.; Gibadulinová, A.; Casini, A.; Cecchi, A.; Scozzafava, A.; Supuran, C. T.; Pastorek, J.; Pastoreková, S. *FEBS Lett.* **2004**, *577*, 439.
10. Chiche, J.; Ilc, K.; Laferrière, J.; Trottier, E.; Dayan, F.; Mazure, N. M.; Brahimi-Horn, M. C.; Pouysségur, J. *Cancer Res.* **2009**, *69*, 358.
11. Supuran, C. T.; Scozzafava, A.; Casini, A. *Med. Res. Rev.* **2003**, *23*, 146.
12. Supuran, C. T. *Nat. Rev. Drug Disc.* **2008**, *7*, 168.
13. Tuccinardi, T.; Nuti, E.; Ortore, G.; Supuran, C. T.; Rossello, A.; Martinelli, A. *J. Chem. Inf. Model.* **2007**, *47*, 515.
14. Briganti, F.; Pierattelli, R.; Scozzafava, A.; Supuran, C. T. *Eur. J. Med. Chem.* **1996**, *31*, 1001.
15. Kim, C.-Y.; Chang, J. S.; Doyon, J. B.; Baird, T. T., Jr.; Fierke, C. A.; Jain, A.; Christianson, D. W. *J. Am. Chem. Soc.* **2000**, *122*, 12125.
16. Alterio, V.; Hilvo, M.; Di Fiore, A.; Supuran, C. T.; Pan, P.; Parkkila, S.; Scaloni, A.; Pastorek, J.; Pastorekova, S.; Pedone, C.; Scozzafava, A.; Monti, S. M.; De Simone, G. *Proc. Natl. Acad. Sci. U.S.A.* **2009**, *106*, 16233.
17. Berman, H. M.; Westbrook, J.; Feng, Z.; Gilliland, G.; Bhat, T. N.; Weissig, H.; Shindyalov, I. N.; Bourne, P. E. *Nucleic Acids Res.* **2000**, *28*, 235.
18. Jones, G.; Willett, P.; Glen, R. C.; Leach, A. R.; Taylor, R. *J. Mol. Biol.* **1997**, *267*, 727.
19. The UniProt Consortium, The Universal Protein Resource (UniProt) in 2010, Nucleic Acids.
20. Bolin, J. T.; Filman, D. J.; Matthews, D. A.; Hamlin, R. C.; Kraut, J. *J. Biol. Chem.* **1982**, *257*, 13650.
21. Studzinski, G. P., Ed.Cell Growth, Differentiation and Senescence: a Practical Approach; Oxford University Press: New York, 1999.
22. Armarego, W. L. F.; Perrin, D. D. *Purification of Laboratory Chemicals*, 4th ed.; Butterworth-Heinemann: Oxford, 1999.
23. (a) Cecchi, A.; Hulikova, A.; Pastorek, J.; Pastorekova, S.; Scozzafava, A.; Winum, J.-Y.; Montero, J.-L.; Supuran, C. T. *J. Med. Chem.* **2005**, *48*, 4834; (b) Casey, J. R.; Morgan, P. E.; Vullo, D.; Scozzafava, A.; Mastrolorenzo, A.; Supuran, C. T. *J. Med. Chem.* **2004**, *47*, 2337.
24. (a) Pastorekova, S.; Casini, A.; Scozzafava, A.; Vullo, D.; Pastorek, J.; Supuran, C. T. *Bioorg. Med. Chem. Lett.* **2004**, *14*, 869; (b) Vullo, D.; Innocenti, A.; Nishimori, I.; Pastorek, J.; Scozzafava, A.; Pastorekova, S.; Supuran, C. T. *Bioorg. Med. Chem. Lett.* **2005**, *15*, 963.
25. Gupta, S. P.; Maheswaran, V.; Pande, V.; Kumar, D. *J. Enzyme Inhib. Med. Chem.* **2003**, *18*, 7.
26. Pettersen, E. F.; Goddard, T. D.; Huang, C. C.; Couch, G. S.; Greenblatt, D. M.; Meng, E. C.; Ferrin, T. E. *J. Comput. Chem.* **2004**, *25*, 1605.
27. Maestro, version 7.5. Schrödinger Inc.: Portland, OR, 2005.
28. Macromodel, version 8.5. Schrödinger Inc.: Portland, OR, 1999.